Transdermal iontophoresis of dopaminergic (pro) drugs : from formulation to in vivo application

Ackaert, O.

6

Controlling the pharmacokinetics and the pharmacodynamic effect of (S)-5-OH-DPAT with transdermal iontophoresis

Oliver W. Ackaert[a*], Jeroen De Graan[b*], Shanna Shi[d], Rob Vreeken[d], Oscar E. Della Pasqua[c,f] , Durk Dijkstra[b], Ben H. Westerink[b,e] , Meindert Danhof[c] and Joke A. Bouwstra[a]

[a]Division of Drug Delivery Technology, Leiden/Amsterdam Center for Drug Research, Leiden, The Netherlands
[b]Department of Medicinal Chemistry, University Center of Pharmacy, University of Groningen, The Netherlands
[c]Division of Pharmacology, Leiden/Amsterdam Center for Drug Research, Leiden, The Netherlands
[d]Division of Analytical biosciences, Leiden/Amsterdam Center for Drug Research, Leiden, The Netherlands
[e]Department of biomonitoring and sensoring, University Center of Pharmacy, University of Groningen, The Netherlands
[f]Clinical Pharmacology and Discovery Medicine, GlaxoSimthKline, Greenford, United Kingdom

[*]Contributed equally as first author
2010. *submitted for publication*

Abstract

The pharmacokinetic (PK) and pharmacodynamic (PD) properties of the active (S)-enantiomer of the potent dopamine agonist 5-OH-DPAT were investigated in a novel anesthetized animal model. Firstly, the relationship between current density, *in vivo* transport and plasma profile was characterized. Secondly, the effect of the anesthetic mixture, transdermal iontophoresis and blood sampling on the striatal dopamine release (PD endpoint) was investigated. Thirdly, the PK-PD relationship following transdermal iontophoresis was investigated during a controlled and reversible pharmacological response. As pharmacodynamic effect the dopamine release in striatum was selected. Given that the striatal dopamine levels are unaltered during experimental procedures, this rat model can be used to investigate the PK-PD relationship. The *in vivo* flux was found to be linearly correlated with the current density, which indicates that drug delivery can carefully be titrated by the current density. Following both transdermal iontophoresis and IV infusion, a strong and reversible PD effect was observed. Compartmental modeling showed that the relationship between drug plasma concentration and biomarker response can be best characterized by an effect compartment, rather than an indirect response model. In addition, covariate analysis suggested that the delivery rate can affect the pharmacodynamic efficiency. Finally, simultaneous PK-PD analysis revealed that steady delivery rates are translated into continuous dopaminergic stimulation. This can be of great benefit for reducing side effects in the symptomatic treatment of Parkinson's disease with 5-OH-DPAT.

Keywords: PK-PD, compartmental modeling, iontophoresis, (S)-5-OH-DPAT, microdialysis

1 Introduction

Transdermal iontophoresis is a well established physical method to facilitate the percutaneous penetration of molecules [1]. By application of a small electrical current across the skin iontophoresis enhances the transdermal delivery of therapeutic agents. An important advantage of transdermal delivery is the circumvention of the hepatic first-pass metabolism, making it an interesting non-invasive alternative for oral drug delivery. A particular advantage of iontophoresis is the possibility to tailor the delivery to the patient's needs by adjusting the current density. This may allow for better therapeutic efficacy and reduction in overdosing and subsequent side effects. These properties make iontophoresis an excellent method for the transdermal delivery of drug molecules for the symptomatic treatment of Parkinson's disease.

Parkinson's disease is a neurodegenerative disorder, which is characterized by tremor, akinesia, rigidity and postural instability [2]. Up to today orally dosed levodopa is still the most effective symptomatic treatment, but chronic use eventually leads to severe long-term side-effects, i.e. dyskinesia and the *on-off* phenomenon [3-4]. Current strategy to prevent or delay the onset of these side-effects is to administer therapeutics in a constant and controlled manner [5]. Therefore, the transdermal iontophoretic delivery of the dopaminergic agonists R-apomorphine, ropinirole and 5-OH-DPAT were investigated *in vivo* for their application in symptomatic treatment of Parkinson's disease [6-9].

Besides a constant and controlled delivery, another attractive property of iontophoresis is the possibility to develop a feedback system. In this approach, the concentration of a relevant biomarker, extracted for instance with reverse iontophoresis, can be used to titrate the transdermal iontophoretic delivery of the drug molecule. Preferably, a pharmacodynamic endpoint instead of the drug plasma concentration should be chosen to monitor the drug effect. Under experimental conditions, striatal dopamine concentration, measured by microdialysis, has been shown to be a biomarker for dopaminergic activity [10-11].

In the current investigation, we have therefore characterized pharmacokinetic-pharmacodynamic (PK-PD) relationships of the dopamine agonist following transdermal iontophoresis using dopamine as a measure of the pharmacological effect. In order to optimize the feedback system, we have also performed an integrated evaluation of relationship between the pharmacodynamics,

pharmacokinetics and the delivery rates of the compound. In a previous study, the PK-PD of 5-OH-DPAT was assessed, however a ceiling effect was observed, with dopaminergic levels not altering throughout the time frame of the experiments [7]. Modelling of the data was therefore difficult and demanded for a follow-up study to investigate the PK-PD relationship under a wider exposure range, in which maximum effect (ceiling) is short lasting. In addition, during the previous study 5-OH-DPAT was administered as racemic mixture, while (S)-5-OH-DPAT is the only enantiomer with dopaminergic activity. In contrast to previous studies, in the present investigation, experiments are conducted with the active enantiomer (S)-5-OH-DPAT [7].

The aims of this study were three-fold. First, to examine the relationship between the current density, the *in vivo* iontophoretic transport and the (S)-5-OH-DPAT plasma profile. Given the requirement for the use of anaesthesia to conduct transdermal iontophoresis, second, to examine the effect of the anesthetic mixture, transdermal iontophoresis and blood sampling on the striatal dopamine release. Third, to assess the PK-PD relationship following transdermal iontophoresis of (S)-5-OH-DPAT,

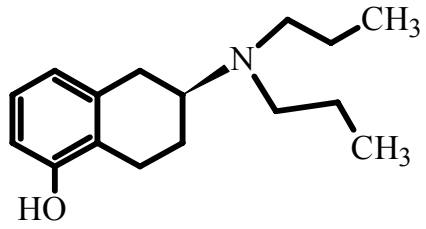

(S)-5-OH-DPAT

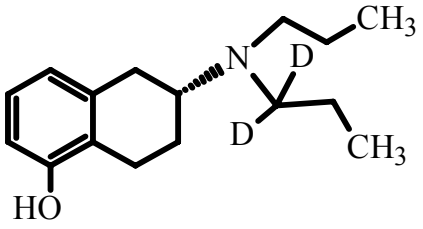

(R)-d_2-5-OH-DPAT

Figure 1: The molecular structures of (S)-5-hydroxy-2-(N,N,-di-n-propylamino)tetralin ((S)-5-OH-DPAT) and (R)-5-hydroxy-2-(N-*n*-propyl-N-α,α-dideutero-propylamino)-tetralin ((R)-d_2-5-OH-DPAT)

ensuring the induction of a controlled and reversible effect [7]. A comprehensive approach based on non-linear mixed effects modeling was used that allows us to characterize and predict the time course of drug action. Furthermore this approach enables to combine data from different experiments to obtain individual and population PK-PD parameter estimates [12]. Extensive PK-PD modeling is further applied to characterize the pharmacokinetics of (S)-5-OH-DPAT in plasma and the corresponding pharmacodynamic effect. The PK model to describe the plasma concentration was adapted from literature [7]. Given that a delay is observed between plasma concentrations and the onset of the pharmacological response, two PD models are compared to describe the DA release: the effect compartment model [13] *vs* the indirect response type I model [14]. The results of this comparison add value to the efforts in the optimization of drug delivery. We ultimately illustrate how PK-PD relationships can be used to design a delivery system for symptomatic treatment of Parkinson's disease.

2 Materials and Methods

2.1 Chemistry

5-hydroxy-2-(N,N,-di-n-propylamino)tetralin ((S)-5-OH-DPAT) and (R)-5-hydroxy-2-(N-*n*-propyl-N-α,α-dideutero-propylamino)-tetralin ((R)-d_2-5-OH-DPAT) (HBr salts, purity > 98%) were synthesized at the Department of Medicinal Chemistry of the University of Groningen, Groningen, the Netherlands (Figure 1). To synthesize d_2-5-OH-DPAT the following deuteration strategy was employed: (+)-5-Methoxy-2-(N-*n*-propylamino)tetralin was converted to the propionamide. Subsequently, the propionamide was reduced with lithium aluminium deuteride and after demethylation with 48% hydrobromic acid, the final compound d_2-5-OH-DPAT hydrobromide was obtained with an overall yield of 13%.

2.2 Materials

Silver, silver chloride (puritiy >99.99%) and octanesulfonic acid were obtained from Sigma-Aldrich (Zwijndrecht, the Netherlands). Acetonitrile (LC-MS grade), ammonium acetate (LC-MS grade), acetic acid (LC-MS grade) and methanol (LC-MS grade) were purchased from Biosolve (Valkenswaard, the Netherlands). Ammonium hydroxide (25% w/v; analytical grade) was obtained from Baker (Deventer, the Netherlands). NaCl 0.9% was purchased from the hospital pharmacy of LUMC (Leiden, the Netherlands). EDTA was obtained from Merck (Merck

KGaA, Darmstadt, Germany). All solutions were prepared in Millipore water with a resistivity of more than 18 MΩ.cm.

2.3 Iontophoresis patches

A detailed description of the iontophoresis patches, used for the transdermal iontophoresis studies can be found elsewhere [7]. Briefly, the iontophoresis patches were prepared by the Fine Mechanical Department of Leiden University from elastic silicon materials (silicon: Smooth-Sil 920; Smooth-on Inc., Easton, PA, USA). The volume of the patches was 2.3 ml and the active area was 2.5 cm². The patch was fixed on wound dressing film (Opsite Flexigrid, Smith&Nephew, Hoofdorp, the Netherlands), which can be attached to the skin during the experiment. Ag/AgCl was used as driver electrode pair.

2.4 Animals

Animal procedures were conducted in accordance with guidelines published in the NIH guide for the care and use of laboratory animals and all protocols were approved by the Institutional Animal Care and Use Committee of the University of Groningen and Leiden University. The pharmacokinetic (PK) and the pharmacokinetic-pharmacodynamic (PK-PD) studies were performed in albino male Wistar rats (280-340 g) obtained from Charles River (Maastricht, the Netherlands) and Harlan (Horst, the Netherlands), respectively. Prior to surgery the animals were housed at least 1 week in Plexiglas cages, maximum 6 animals per cage with free access to water and standard laboratory chow. The cages were placed in a room with a controlled temperature at 21 °C and controlled humidity between 60-65% and a light-dark cycle of 12h.

2.5 Pharmacokinetic (PK) studies

In these experiments the relationship between the current density and the plasma concentration profile of (S)-5-OH-DPAT following transdermal iontophoresis was investigated. (S)-5-OH-DPAT was administered by transdermal iontophoresis and intravenous (IV) infusion to the same animals with a one week interval between treatments. The use of both routes of administration allowed improved pharmacokinetic parameter estimation. A detailed description of the experiments is given below.

2.5.1 Surgical procedures

Prior to surgery the animals were anaesthetized with a combination of Dormicum® (midazolam, 5 $mg.ml^{-1}$, Roche Nederland, Mijdrecht, the Netherlands) and Hypnorm® (fentanyl citrate 0.315 $mg.ml^{-1}$ + fluanizone 10 $mg.ml^{-1}$, Janssen Pharmaceutica, Beerse, Belgium) at a dose of 0.5 $mL.kg^{-1}$ rat weight. The permanent cannulation was performed using Polethene tubings (Rubler BV, Hilversum, the Netherlands) with the diameter of 0.58 mm (I.D.) – 0.96 mm (O.D.) and 0.28 mm (I.D.) – 0.61 mm (O.D.), respectively for femoral vein and artery cannulation. After surgery the animals were housed individually and were allowed to recover during one week.

2.5.2 Experimental procedures

In the first part of the study (S)-5-OH-DPAT was administered by transdermal iontophoresis. Firstly the animals were anesthetized with Hypnorm® and Dormicum® (0.5 $mL.kg^{-1}$) and the hair of the back was removed using an electrical clipper and a scalpel. A pair of patches was attached to the skin surface. After 15 min the patches were filled with (S)-5-OH-DPAT (3.9 mM) at pH 5.0 (citric buffer, 5 mM) and with PBS pH 7.4 (NaCl: 8 $g.L^{-1}$, Na_2HPO_4: 2.86 $g.L^{-1}$, KH_2PO_4: 0.2 $g.L^{-1}$, KCl: 0.19 $g.L^{-1}$) at the anodal and the cathodal side, respectively. The following protocol was used for the iontophoresis studies: 15 min passive diffusion + 120 min 75 $\mu A.cm^{-2}$ + 120 min 150 $\mu A.cm^{-2}$. At time=255 min, the patches were removed and the skin was wiped using a tissue paper. Blood samples were taken at regular time intervals during the current application and after removal of the patch: 0, 15, 45, 75, 105, 135, 165, 195, 225, 255, 270, 285, 315, 345, 390, 435 min. Blood samples (0.2 ml) were collected using lithium-heparin containing tubes (Microvette® 200 Plasma/Lithium Heparin, Sarsted BV, Etten-Leur, the Netherlands). Plasma was then separated by centrifugation at a speed of 6000 rpm during 10 min. The samples were kept at -20 °C prior to analysis with LC-MS-MS (section 2.7).

After 1 week of recovery in individualized housing, animals received a total dose of 29 nmol (S)-5-OH-DPAT, dissolved in 0.9% NaCl, during a 15-min IV infusion. At regular time intervals blood samples were taken from the femoral artery cannula: 0, 15, 20, 30, 45, 60, 75, 90, 105, 120, 150, 180 min. The samples were prepared in the same way as described above following iontophoretic delivery (see above). In all experiments the animals were kept in an anaesthetized condition during the experiment using Hypnorm® and Dormicum®.

2.6 On-line microdialysis studies (PK-PD studies)

This series of experiments consisted of three parts. Firstly, the influence of anesthesia and iontophoresis on the striatal dopamine release (PD end point) was determined with on-line microdialysis. Secondly, the pharmacokinetic (PK) and pharmacodynamic (PD) properties following transdermal iontophoretic delivery were examined. Thirdly, to explore the implications of differences in delivery rate on the PK and PD parameters, (S)-5-OH-DPAT was administered with IV infusion. In all experiments the striatal dopamine level and the striatal 5-OH-DPAT concentration were monitored by microdialysis with simultaneous blood sampling for the analysis of (S)-5-OH-DPAT plasma concentrations. A detailed description of the experiments is given below.

2.6.1 Surgical procedures

Prior to surgery the rats were anaesthetized with Isofluran 2% in N_2O/O_2 (2/1). The permanent cannulations were performed using silicone catheters (inner diameter (I.D.): 0.5 mm; outer diameter (O.D.): 0.9 mm) (UNO BV, Zevenaar, The Netherlands). The catheters were inserted approximately 2 cm inside the vessels. The catheters were tunneled subcutaneously, externalized at the back of the head. After the cannulation the rats were kept under anaesthetized condition and mounted into a stereotaxic frame for the implementation of microdialysis probes in left and right striatum according to a method described previously [10-11]. After exposing and anesthetizing the skull with 0.5% marcaine-adrenaline, the holes for probe insertion were drilled. A Y-shaped dialysis probe was used for the experiments, with an exposed tip length of 3 mm. The dialysis cannula (I.D.: 0.24 mm; O.D.: 0.34 mm) was prepared from polyacrylonitrile/sodium methallyl sulfonate copolymer (AN 69, Hospal, Bologna, Italy). The microdialysis cannula was implanted in the striatum. The following coordinates were used according to the atlas of Paxinos and Watson [15]: AP +0.9, LM ± 3.0 relative to bregma, and Vd – 6.0 below dura. Before insertion into the brain, the dialysis probe was perfused successively with 70% ethanol, ultrapure water and Ringer solution (140 mM NaCl, 3.0 mM KCl, 1.2 mM $CaCl_2$, 1.0 mM $MgCl_2$). The dialysis probe was positioned in the burr hole under stereotaxic guidance. The probe was cemented in this position with dental cement. Thereafter the rats were housed solitary.

2.6.2 Experimental procedures

The PK-PD experiments were performed 15-20 h after cannulation and implantation of the probes. The rats were anaesthetized prior to and kept under anesthetized

condition during the experiment with Hypnorm® and Dormicum® at a starting dose of 0.5 mL.kg^{-1} and subsequently with hourly doses of 0.17 mL.kg^{-1}.
Firstly, to dismiss the potential confounding effects of anaesthesia, an iontophoretic control experiment was conducted administering only citric buffer (pH 5.0, 5 mM), as this is the donor phase used for transdermal iontophoresis, without (S)-5-OH-DPAT. Before the start of the experiment, the hair of the back of the anesthetized rat was removed with an electrical clipper and scalpel. 15 min after attaching the patches to the skin surface, the cathodal patch was filled with PBS pH 7.4 and the anodal patch was filled with the donor solution. The protocol for iontophoresis was: 15 min passive diffusion + 90 min current application (250 µA.cm^{-2}). The patch was removed and the skin was wiped using tissue paper. To include the influence of blood sampling on the DA level, blood samples were taken at regular time intervals: 0, 15, 30, 45, 60, 75, 90, 105, 120, 135, 165, 195, 225, 255, and 285. Blood sampling and subsequent preparation of the samples were identical to the procedures used for the PK studies following transdermal iontophoresis (*cf*. supra).

Secondly, a PK-PD microdialysis study following transdermal iontophoretic delivery of (S)-5-OH-DPAT was performed. The donor solution consisted of (S)-5-OH-DPAT (3.9 mM), buffered with a citric buffer (pH 5.0, 5 mM). All the experimental procedures were identical to the control experiment, as described in the previous paragraph. Thirdly, a PK-PD microdialysis study was performed with a total dose of 113 nmol 5-OH-DPAT, dissolved in NaCl 0.9%, administered as a 10-min IV infusion. Blood sampling and subsequent preparation of the samples were identical to the procedures used for the PK studies following IV infusion (*cf*. supra).

In all the PK-PD studies the dopamine level and the 5-OH-DPAT concentration were monitored in the left and right striatum, respectively, with microdialysis. The microdialysis probes in the striata were perfused with Ringer solution at a flow of 2 µL.min^{-1} (CMA/102 Microdialysis Pump, Sweden). Every 15 min a sample was collected for analysis with a total volume of 30 µl. The analysis of the microdialysate samples is described below (section 2.7.2).

2.7 Sample analysis

2.7.1 Blood samples of (S)-5-OH-DPAT

The blood samples of 5-OH-DPAT were analyzed with an on-line solid-phase extraction-liquid-chromatography-mass spectrometry/mass spectrometry (SPE-LC-MS/MS) method. 5 µl of the internal standard (d_2-5-OH-DPAT; 5 ng.ml^{-1}) was added to 35 µl of the collected plasma and 350 µl acetonitrile was added to precipitate the

proteins. The mixture was vortexed and centrifuged at a speed of 8000 rpm during 10 min at 10 °C. The supernatant was dried and redissolved in 50 µl MilliQ and 3 µl was injected on to the SPE cartridge. An external binary HPLC pump (Gynkotek, Munich, Germany) and an external Agilent 1200, 2/6 switch valve (Agilent Technology, Santa Clara. CA, USA) were used for the SPE sample trapping. The samples were trapped on a Hysphere Resin C8, endcapped, 10 x 4 mm, 10 µm SPE cartridge (Spark Holland B.V, Emmen, The Netherlands). Prior to injection, the SPE cartridge was conditioned with 50mM ammonium acetate buffer pH 9.0, after the injection the sample was trapped with 10mM ammonium acetate buffer pH 9.0/ACN (4:1 v/v) during 1 min with a flow of 0.4 $ml.min^{-1}$. Subsequently, the valve was switched placing the SPE cartridge in-line with the LC system for elution onto the analytical column. Elution of 5-OH-DPAT and its internal standard was accomplished by flushing the SPE column with H_2O/ACN (1:9 v/v) during 4 min with a flow of 0.05 $ml.min^{-1}$ and 1 min with 1 $ml.min^{-1}$. Finally, the cartridge was switched off-line again and re-conditioned using a 50mM ammonium acetate buffer at pH 9.0 during 2 min with a flow of 1 $ml.min^{-1}$. To analyze the extracted sample an Agilent 1200 HPLC system with autosampler (Agilent Technology, Santa Clara. CA, USA) was coupled online with an Agilent 6460 Triple Quadrupole mass spectrometer (Agilent Technology, Santa Clara. CA, USA). The samples were analyzed by µPLC-MS/MS using an Altima HP C18 column (150X 1.0 mm; 5 µm) (Grace Davison Discovery Sciences, Lokeren, Belgium). The mobile phase consisted of 10 mM ammonium acetate buffer pH 3.7: Acetonitril (2.3:1 v/v) was used. The total analysis time was 11 min, the flow-rate was 100 $\mu l.min^{-1}$, the temperature of the autosample tray was set to 4 ºC and the column temperature was set to room temperature. The detection was performed with a triple quadrupole mass spectrometer in the positive-ion electrospray mode and all analytes were monitored with Multiple Reaction Monitoring (MRM). 5-OH-DPAT and the internal standard d_2-5-OH-DPAT were ionized to produce the protonated molecules at m/z 248 and m/z 250, respectively. Upon collision (collision energy 15 eV; fragmentor enenergy 120 V) the pre-cursor ions of both of 5-OH-DPAT and d_2-5-OH-DPAT produced the same product-ion at m/z 147, corresponding to 5-hydroxy-aminotetraline. System operation and handling the acquired data was performed using Agilent MassHunter data acquisition software (version, B.02.00; Agilent). Calibration curves showed a linear response when using concentrations of compounds between 0.2 and 50 $ng.ml^{-1}$ (R^2>0.999). The recovery, limit of detection (LOD) and limit of quantification (LOQ) were experimentally determined at 93.9 ± 2.9 %, 0.07 and 0.2 $ng.ml^{-1}$, respectively.

2.7.2 Microdialysate samples of (S)-5-OH-DPAT

To analyze the striatal 5-OH-DPAT concentration the dialysate from the probe in the right striatum was collected every 15 min, resulting in a total volume of 30 µL per sample. Subsequently, 70 µL of a 7.15 nM solution of (R)-d_2-5-OH-DPAT as internal standard was added to yield final concentrations of 5 nM internal standard in a 100 µL mixture of water + 0.1% formic acid and Ringer (1:1). The solution was analyzed using LC-MS/MS. The HPLC system consisted of a Shimadzu LC 20 AD binary system with a Shimadzu SIL 20AC autosampler. The samples were injected on a Grace Alltech Alltima HP C18 EPS reverse-phased column (3 µm, length 150 x 2.1 mm I.D.) (Grace Alltech, Lokeren, Belgium). The mobile phase consisted of a mixture of 0.1% formic acid in water (solvent A) and 0.1% formic acid in acetonitrile (solvent B). The gradient was programmed as follows: 1 minute isocratically at 15% B, increase in 7.5 min to 95% B, 2.5 min isocratically at 95% B, decrease in 1 minute to 15% B and isocratically for 5 min at 15% B. The total runtime was 17 min. The flow was set at 0.4 $mL.min^{-1}$ and the analysis was performed at room temperature. The injection volume was 20 µL (partial loop fill) and the compounds were detected on a SCIEX API3000 triple quadrupole mass spectrometer (Applied Biosystems/MDS SCIEX, Foster City, CA, USA) equipped with a Turbo Ion Spray interface. The mass spectrometer was operated in the positive ion mode with MRM, quantifying transition pairs of m/z 248.2/147.1 and 250.2/147.1 for 5-OH-DPAT and d_2-5-OH-DPAT, respectively. Instrument parameters were as follows: Ion spray voltage 5000 V, nebulizer gas 13, curtain gas 13, TIST (Turbo Ion Spray Temperature) 500 °C, collision activated dissociation (CAD) gas 4, declustering potential (DP)=35 V, focusing potential (FP)=130 V, entrance potential (EP)=10 V. The detection limit of 5-OH-DPAT was 1 fmol which is 0.25 pg (5×10^{-11} M, 20 µL injection volume).

2.7.3 Striatal concentration of dopamine (DA) and metabolites

The dialysate contents of dopamine (DA) and its metabolites were quantified from the probe implanted at the left striatum by an on-line HPLC with electrochemical detection with the detection limit of 1 fmol/sample. A HPLC pump (LC-10AD vp, Shimadzu, Kyoto, Japan) was used in conjunction with an analytical cell (5011A, ESA, Chelmsford, MA, USA) and a electrochemical detector (Coulochem II, ESA, Chelmsford, MA, USA) working at +300 mV for DOPAC and HIAA and -300 mV for DA. The analytical column was a Supelco Supelcosil™ LC-18-DB column (150 mm x 4.6 mm, 3 µm) (Sigma-Aldrich Chemie B.V., Zwijndrecht, The Netherlands). The mobile phase consisted of a mixture of 4.1 g.L-1 sodium acetate (Merck), 215

mg.L^{-1} octane sulphonic acid, 186 mg.L^{-1} EDTA, 7% methanol and ultrapure water (pH=4.2 with glacial acetic acid). Data were converted into percentage of basal levels. The basal levels were determined from four consecutive samples (less than 20% variation), and set to 100%. After the experiments the rats were sacrificed and the brains were removed. The brains were kept in 4% paraformaldehyde solution until they were sectioned to control the location of the dialysis probes.

2.8 Data analysis

A non-linear mixed effects modeling approach was used to describe the pharmacokinetics of (S)-5-OH-DPAT in plasma and the dopamine levels (PD endpoint) in the striatum. The *in vivo* data following transdermal and IV infusion were combined for analysis.

2.8.1 PK model

A detailed description of the pharmacokinetic model for (S)-5-OH-DPAT has been reported elsewhere [7]. Briefly, the PK model is based on compartmental mass transfer to describe the iontophoretic transport *in vivo*. Data fitting was performed according to the ordinary differential equations 1, 2 and 3 for transdermal iontophoretic delivery:

$$\frac{dX_1(t)}{dt} = I_0.N - K_R.X_1(t) \quad (1)$$

$$\frac{dX_2(t)}{dt} = K_R.X_1(t) - k.X_2(t) - k_{23}.X_2(t) + k_{32}.X_3(t) \quad (2)$$

$$\frac{dX_3(t)}{dt} = k_{23}.X_2(t) - k_{32}.X_3(t) \quad (3)$$

With $\frac{dX_i(t)}{dt}$ as the rate of change in the amount of the drug in compartment *i*, X_i as the amount of the drug in compartment *i*, which refers to the skin compartment (*i*=1), the plasma compartment (*i*=2) and the peripheral compartment (*i*=3). I_0 is defined as the zero order mass input during iontophoresis, K_R as the first order release rate constant from skin to plasma, *k* as the first order elimination rate constant, k_{23} and k_{32} as the first order distribution rate constants from plasma to tissue and tissue to plasma, respectively. N is a flag in the model to indicate that the input rate I_0 is only valid during the iontophoresis period.

Following intravenous administration, data was modeled using Equation 4, which describes the rate of change in amount of the drug in the plasma compartment:

$$\frac{dX_2(t)}{dt} = Rate.M - k.X_2(t) - k_{23}.X_2(t) + k_{32}.X_3(t) \tag{4}$$

With *Rate* as the zero order intravenous infusion rate and *M* as a flag to indicate that the *Rate* only applies during the duration of the infusion. Equation 3 was used to describe the rate of change in the peripheral compartment.

2.8.2 PD model

Two PD models were compared to fit the data of the dopamine release in the striatum during and after transdermal iontophoresis and intravenous infusion. The first model was the indirect response (IDR) type I model in analogy to the model proposed by Nugroho *et al.* [7]. The levels of 5-OH-DPAT in the plasma (C_p) were directly linked to the dopaminergic effect. The equations of the model to describe the rate of change in the dopamine concentration $\frac{dC_{DA}(t)}{dt}$ in the striatum:

$$\frac{dC_{DA}(t)}{dt} = k_{in}^0.\left(1 - \frac{I_{\max}.C_p(t)^H}{IC_{50} + C_p(t)^H}\right) - k_{out}.C_{DA}(t) \tag{5}$$

$$k_{in}^0 = k_{out}.C_{DA}(0) \tag{6}$$

With I_{max} as the maximum inhibition of the dopamine production, IC_{50} is the plasma concentration of 5-OH-DPAT at which 50% of maximum inhibition is observed, *H* is the slope of the curve (Hill coefficient), k^0_{in} is the zero order rate constant for the production of response, k_{out} is the first order rate constant for the loss of response, $C_{DA}(0)$ is the baseline values of dopamine (i.e., dopamine concentration prior to the inhibiting effect of 5-OH-DPAT).

In the second model, an extra hypothetic compartment was introduced to account for the delay between plasma concentration and the response, i.e., the effect compartment. The rate of change of drug concentration $\frac{dC_e(t)}{dt}$ in the effect compartment can be described as follows:

$$\frac{dC_e(t)}{dt} = k_{e0}.\left(C_2(t) - C_e(t)\right) \tag{7}$$

With k_{e0} as the first order distribution rate constant from plasma to effect compartment and the elimination rate constant from the effect compartment. The effect is described by the sigmoid I_{max} model using the following equation:

$$C_{DA} = C_{DA}(0).\left(1 - \frac{I_{\max}.C_e(t)^H}{IC_{50}{}^H + C_e(t)^H}\right) \quad (8)$$

With C_e as the drug concentration in the effect compartment.

2.8.3 Model parameters

A detailed description of the PK and PD modeling steps is presented elsewhere [7]. In short, the data analysis was performed using NONMEM version VI (NONMEM project group, University of California, San Francisco, USA), using the ADVAN6 TRANS1 TOL=5 from PREDPP, as subroutines. The fixed effect parameters (θ) included: I_0, K_R, clearance (CL), inter compartmental clearance (Q), volume of the central compartment (V_2), volume of the peripheral compartment (V_3), k_{out}, I_{max}, IC_{50} and k_{e0}. Variability in pharmacokinetic parameters was assumed to be log-normally distributed in the population. Inter-individual variability was modeled by an exponential error model as written in Equation 9:

$$P_i = \theta.\exp(\eta_i) \quad (9)$$

in which θ is the population value for the fixed effect parameter P, P_i is the individual estimate and η_i is the normally distributed interindividual random variable with mean zero and variance ω^2. The coefficient of variation (CV %) of the structural model parameters is expressed as percentage of the root mean square of the interindividual variability term. The residual error was modeled by a proportional error model as written in Equation 10:

$$C_{obs,ij} = C_{pred,ij}.(1 + \varepsilon_{ij,1}) \quad (10)$$

where $C_{obs,ij}$ is the jth observed concentration in the ith individual, $C_{pred,ij}$ is the predicted concentration, and ε_{ij} is the normally distributed residual random variable with mean zero and variance σ^2. The estimation of the final population parameters was performed using the conventional first order estimation method (FOCE). The PK model parameters were estimated independently and subsequently used as input for the PD analysis. During model building, goodness-of-fit was based on statistical and graphical diagnostic criteria. Model selection and identification was based on the

likelihood ratio test, coefficient of variation of parameter estimates, parameter correlations and goodness-of-fit plots. For the likelihood ratio test, the significance level for the inclusion of one parameter was set at $p<0.05$, which corresponds with a decrease of 3.84 points in the minimum value of the objective function (MVOF) under the assumption that the difference in MVOF between two nested models is χ^2 distributed. Non-nested models are evaluated using the Aikaike Information Criterion (AIC), which is the MVOF plus two times the number of parameters. The following goodness-of-fit plots were subjected to visual inspection to detect systemic deviations from the model fits: individual observed versus population and individual predicted values. Finally, the performance of the population PK and PK-PD models were assessed by simulating 100 data sets with the final model parameter estimates. The evaluation of model performance also included visual predictive check (VPC), as implemented in Xpose 4 (R version 2.7.0, R-foundation) [16].

3 Results

Three series of *in vivo* experiments were conducted to investigate the controllability of transdermal iontophoresis and to explore the potential impact of delivery rate on the PK-PD relationship of (S)-5-OH-DPAT. In the first study, the influence of the current density on drug pharmacokinetics in plasma profile was assessed. Two current densities were applied consecutively for 2h (75 and 150 $\mu A.cm^{-2}$). In addition, (S)-5-OH-DPAT was administered as an IV infusion to the same animals to discriminate delivery-related properties from intrinsic pharmacokinetic properties. The crossover design also allowed higher precision of the parameter estimates. In the second study, the influence of the anesthetics, iontophoresis and blood sampling on the striatal dopamine level (PD endpoint) was investigated as a validation procedure for this experimental model. In the third study, the PK-PD relationship was investigated across a range of exposures, with maximum effects being attained for a short period followed by return of DA levels back to baseline conditions. For this reason, transdermal iontophoresis (250 $\mu A.cm^{-2}$) was applied up to 1.5h. In analogy to the first study presented above, (S)-5-OH-DPAT was also administered with IV infusion to enable separation of delivery-related properties from intrinsic pharmacokinetic properties.

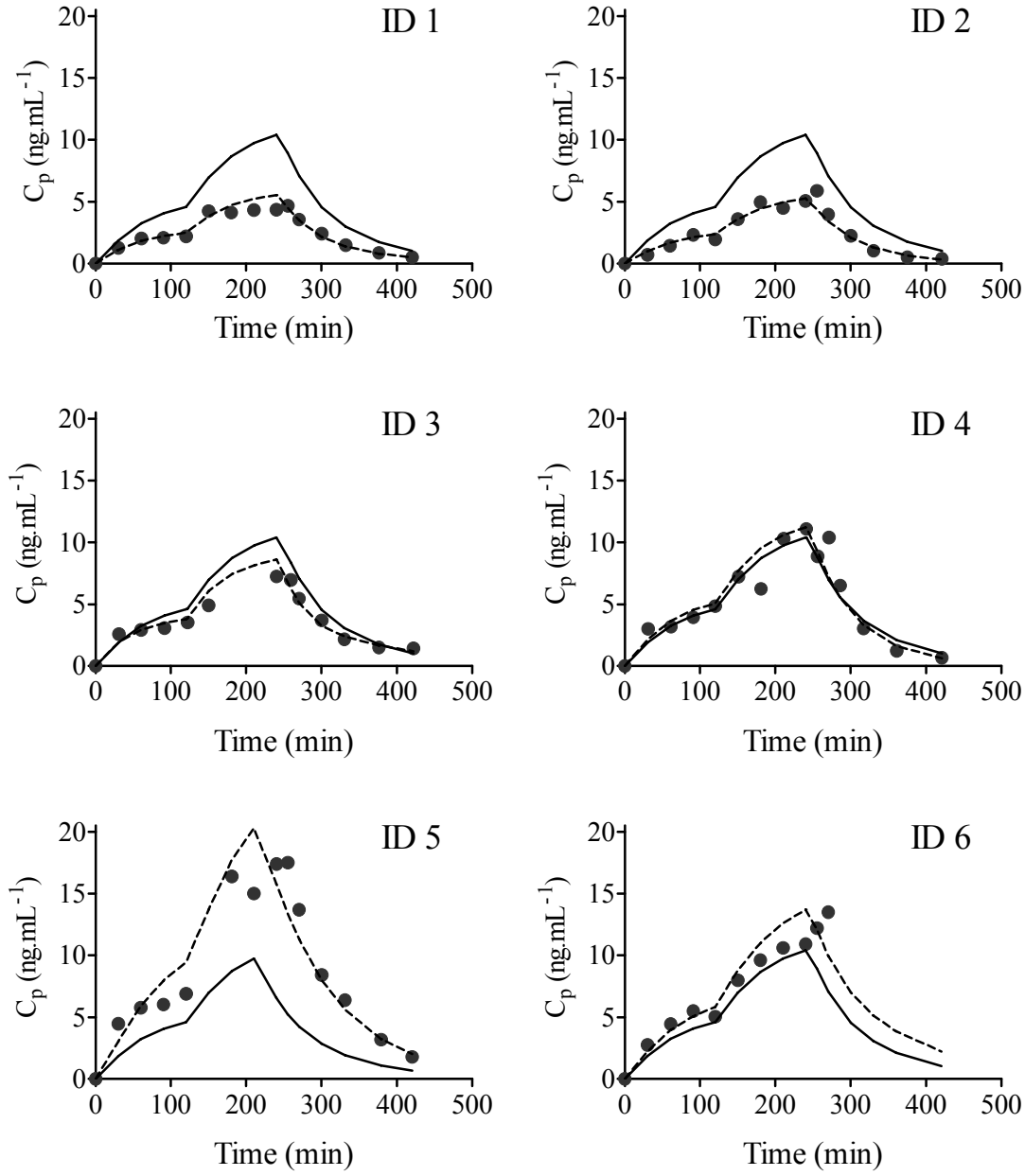

Figure 2: The observed data (filled circles) of the plasma concentration (C_p) of the individual rats during and after transdermal iontophoretic delivery of (S)-5-OH-DPAT (3.9 mM) together with the population model prediction (solid line) and the individual model prediction (dashed line). The following protocol was used: 120 min current density of 75 $\mu A.cm^{-2}$+ 120 min current density of 150 $\mu A.cm^{-2}$. The patch was removed after 240 min

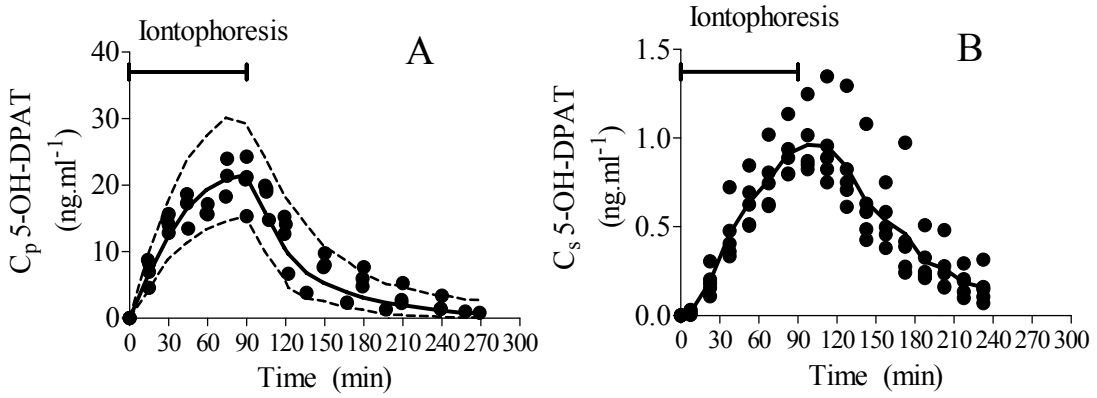

Figure 3: **A**: (S)-5-OH-DPAT concentration-time profiles in blood plasma following transdermal iontophoresis of (S)-5-OH-DPAT (3.9 mM). Depicted are the observed data (filled circles) together with simulated median (50%, solid line) and the upper and lower limit of the model-simulated interquantile concentration range (97.5%-5%, dashed lines).
B: (S)-5-OH-DPAT concentration-time profiles in striatum following transdermal iontophoresis of (S)-5-OH-DPAT (3.9 mM). Depicted are the observed data together with the mean.

3.1 PK properties following iontophoresis and IV infusion

In these studies two different current densities (75 and 150 μA.cm^{-2}) were applied consecutively during 2h to investigate the impact of flux on plasma profiles. Moreover it was of interest to determine the time to reach steady state conditions. The results of the pharmacokinetic studies are depicted in Figure 2. After 15 min of passive diffusion prior to iontophoresis no detectable amount was transported into the plasma (data not shown). In contrast, drug plasma levels increase immediately when switching on the current. In almost all the animals steady state plasma levels were achieved after 2h of 75 μA.cm^{-2} current application, with an average plasma concentration (C_p) of 4.1 ± 1.9 ng.ml^{-1}. By further increasing the current density to 150 μA.cm^{-2}, C_p increased to 9.4 ± 4.8 ng.ml^{-1} after 2h approximately. In parallel, following IV infusion, C_p reached a maximum of 5.3 ± 0.5 ng.ml^{-1} after 15 min (data

not shown). After the discontinuation of infusion or upon termination of the current application, the C_p declined according to a 2-compartment disposition model.

3.2 Validation of the rat model to investigate the PD effect

The potential effects of anaesthesia (fentanyl+fluanisone and midazolam), of blood sampling and of transdermal iontophoresis on the striatal levels of dopamine (PD end-point) were investigated. The results of this control experiment are presented in Figure 4A. Dopamine levels remained stable in the period immediately before attaching the patch (-60 to -15 min) and in the 15 minute period of passive diffusion before iontophoresis (-15 to 0 min). The DA levels, which were set to 100% showed a non-significant small increase from 97 ± 3% to 100 ± 4% during iontophoresis, followed by a stronger increase to 114 ± 6% during 115 min after the end of iontophoresis. These results indicate the suitability of the anesthetized rat model for monitoring of DA levels to evaluate the properties of transdermal iontophoretic delivery or IV infusion of (S)-5-OH-DPAT.

3.3 PK-PD relationships following iontophoresis and IV infusion

The pharmacokinetics and pharmacodynamics of (S)-5-OH-DPAT were assessed following transdermal iontophoresis and IV infusion. With regard to the PK, no detectable plasma concentration could be observed after 15 min passive diffusion (data not shown). When starting the current application (250 $\mu A.cm^{-2}$) the plasma concentration increased immediately and tended towards steady state after 90 min of current application (Figure 3A). The average concentration after 90 min of iontophoresis was 20.4 ± 3.7 $ng.ml^{-1}$. Following IV infusion, C_p reached a maximum of 29.9 ± 2.4 $ng.ml^{-1}$ after 10 min (data not shown). The decline in plasma concentration post (S)-5-OH-DPAT administration was best described by a 2-compartment disposition model. Following transdermal iontophoresis, (S)-5-OH-DPAT concentrations in the striatum were also monitored. As shown in Figure 3B, 5-OH-DPAT concentrations increased to 0.96 ± 0.18 $ng.ml^{-1}$ during current application, but this effect occurred after a small delay (between 7.5 and 22.5 min) in relation to the beginning of iontophoresis. The concentrations decreased again with the same delay upon discontinuation of the iontophoretic current.

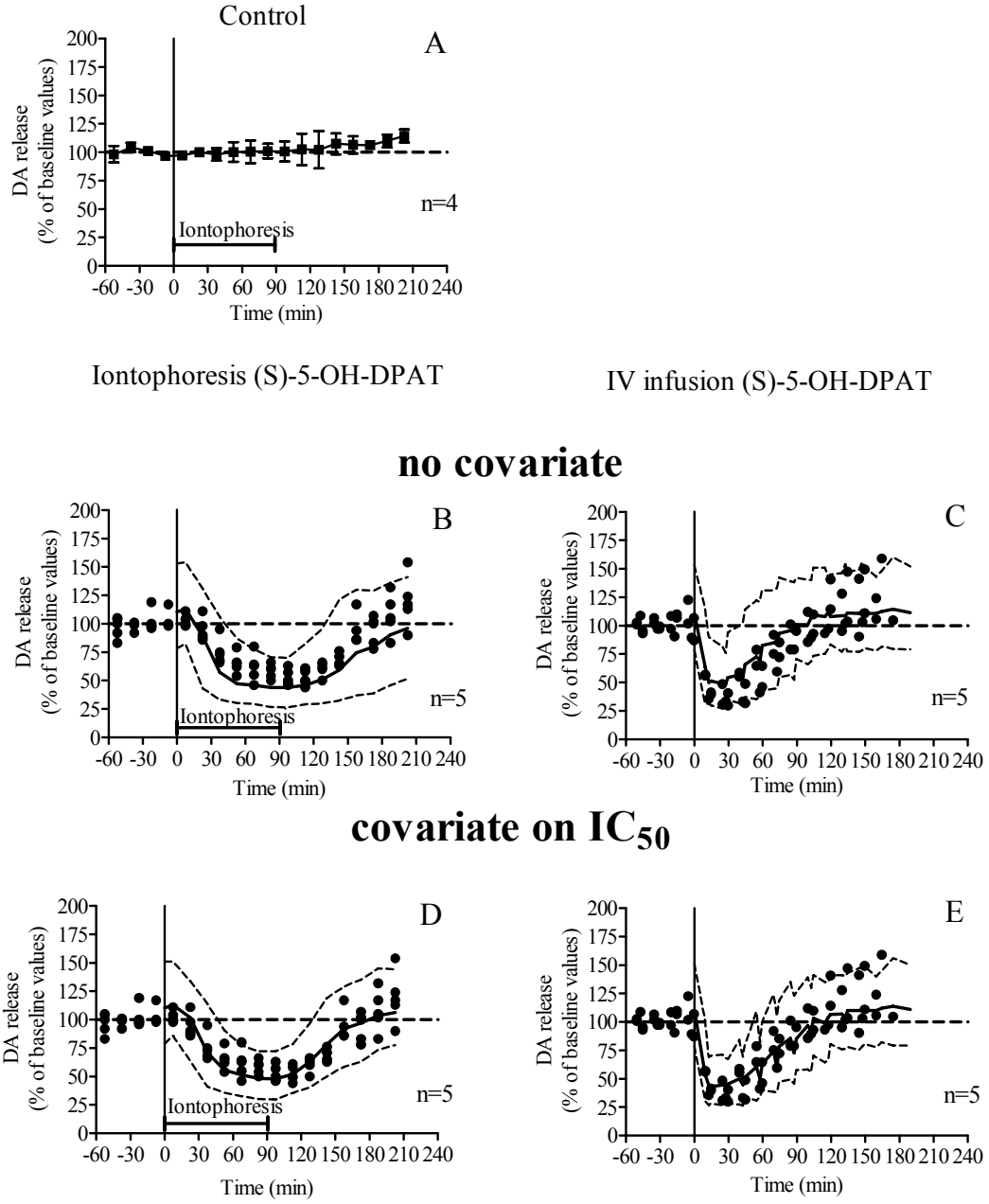

Figure 4: The dopamine release, expressed as % of baseline *vs* time. **A**: transdermal iontophoresis of only buffer (control experiment) **B, D**: transdermal iontophoresis of (S)-5-OH-DPAT (3.9mM).**C, E**: IV infusion of (S)-5-OH-DPAT (113 µM).
A: depicted is the mean ± SD. **B-E**: depicted are the observations (filled circles) together with the model simulated interquantile DA% range (2.5 %-97.5%, dashed lines) and the simulated median (50%, solid line). A number of 100 samples were simulated based on the final parameter estimates.
B, **C**: the visual predictive check without including a covariate of route of administration on IC_{50}. **D**, **E**: the visual predictive check including a covariate of route of administration on IC_{50}. In all panels the average dopamine release of 4 consecutive points prior to administration (time=-60 to -15 min) was set to 100%.

Table 1: The population estimates obtained from fitting the plasma profile and/or the pharmacological response following transdermal iontophoresis. During the PK study, two different current densities (75 and 150 µA.cm^{-2}) were applied consecutively for 2h. During the PK-PD study, a current density of 250 µA.cm^{-2} was applied for 1.5h.

		PK study				**PK-PD study**			
		Estimate		**Between animal variabity**		**Estimate**		**Between animal variabity**	
parameter	unit	mean	RSE %	mean	RSE %	mean	RSE %	mean	RSE %
V_2	L	0.5	6			0.5	18	0.100	71
V_3	L	1.7	16	0.189	46	0.7	16	0.109	42
CL	L.h^{-1}	2.6	13	0.194	45	2.0	6	0.027	29
Q	L.h^{-1}	2.5	9			1.9	23	0.218	44
J_{ss} 75	nmol.cm^{-2}.h^{-1}	24.7	29						
J_{ss} 150	nmol.cm^{-2}.h^{-1}	51.3	30						
J_{ss} 250	nmol.cm^{-2}.h^{-1}					87.3	8	0.000	/
K_R	h^{-1}	2.2	21			5.5	26	0.000	/
k_{e0}	h^{-1}					3.9	10	0.192	77
IC_{50} IONTO	ng.ml^{-1}					4.4	13	0.162	50
IC_{50} IV	ng.ml^{-1}					1.9	11		
N						3.2	10	0.000	/
I_{MAX}	DA%					41.6	8	0.045	36
Sigma PK		0.037	12			0.0246	20		
Sigma PD						0.0120	22		

The striatal dopamine release (PD endpoint) was monitored on-line simultaneously with plasma and striatal concentrations of (S)-5-OH-DPAT. These results are presented in Figure 4. Firstly, the pharmacodynamic effect was monitored following iontophoresis (15 min passive diffusion + 90 min of iontophoresis 250 $\mu A.cm^{-2}$) (Figure 4B). During passive diffusion (-15 to 0 min) no change in DA levels were observed. Subsequently, dopamine levels gradually decreased to a minimum of 48.8 ± 5.1% of basal values within 94.5 ± 16.4 min after the start of the iontophoresis. DA levels returned to baseline values within 79.4 ± 11.3 min after the end of iontophoresis. In contrast, IV infusion of (S)-5-OH-DPAT resulted in an immediate decrease in the DA level. Maximum inhibition of 38.3 ± 8.4 % relative to baseline values was achieved after 42.1 ± 2.5 min (t_{max}) after start of IV infusion (Figure 4C). DA levels returned to baseline values within 120.4 ± 20.5 min after the end of infusion. A slight rebound effect was observed at the end of the experiment. DA level further increased to 119 ± 22 and 120 ± 23% relative to baseline after transdermal delivery and IV infusion, respectively.

3.4 PK-PD analysis following transdermal iontophoretic delivery and IV infusion

The pharmacokinetic data following transdermal iontophoresis was analyzed simultaneously with the PK data following intravenous infusion. The objective of the integrated analysis was to facilitate discrimination between delivery-specific parameters (I_0, K_R) and drug-specific parameters (V_2, V_3, CL, Q). The larger sample size also allowed for more precise estimation of model parameters. The resulting parameters are provided in Table 1. The low relative standard error (RSE) for all the fixed effect parameters (RSE ≤ 30%) indicates high precision of estimates. Moreover, as observed in Figure 2 and in Figure 5A, the model accurately describes the time course of plasma concentration during and after current application.

An integrated approach was also applied to the PK-PD experiments. The analysis of the PK PD data following IV administration and iontophoresis was performed simultaneously. In analogy to the PK study, the plasma concentration profile could be described by the proposed compartmental model. In Figure 3A, the VPC depicts the goodness of fit, with observed data randomly distributed within the 95% confidence interval (C.I.). In addition, the diagnostic plots (Figure 5B) show a good correlation between the observed and predicted C_p.

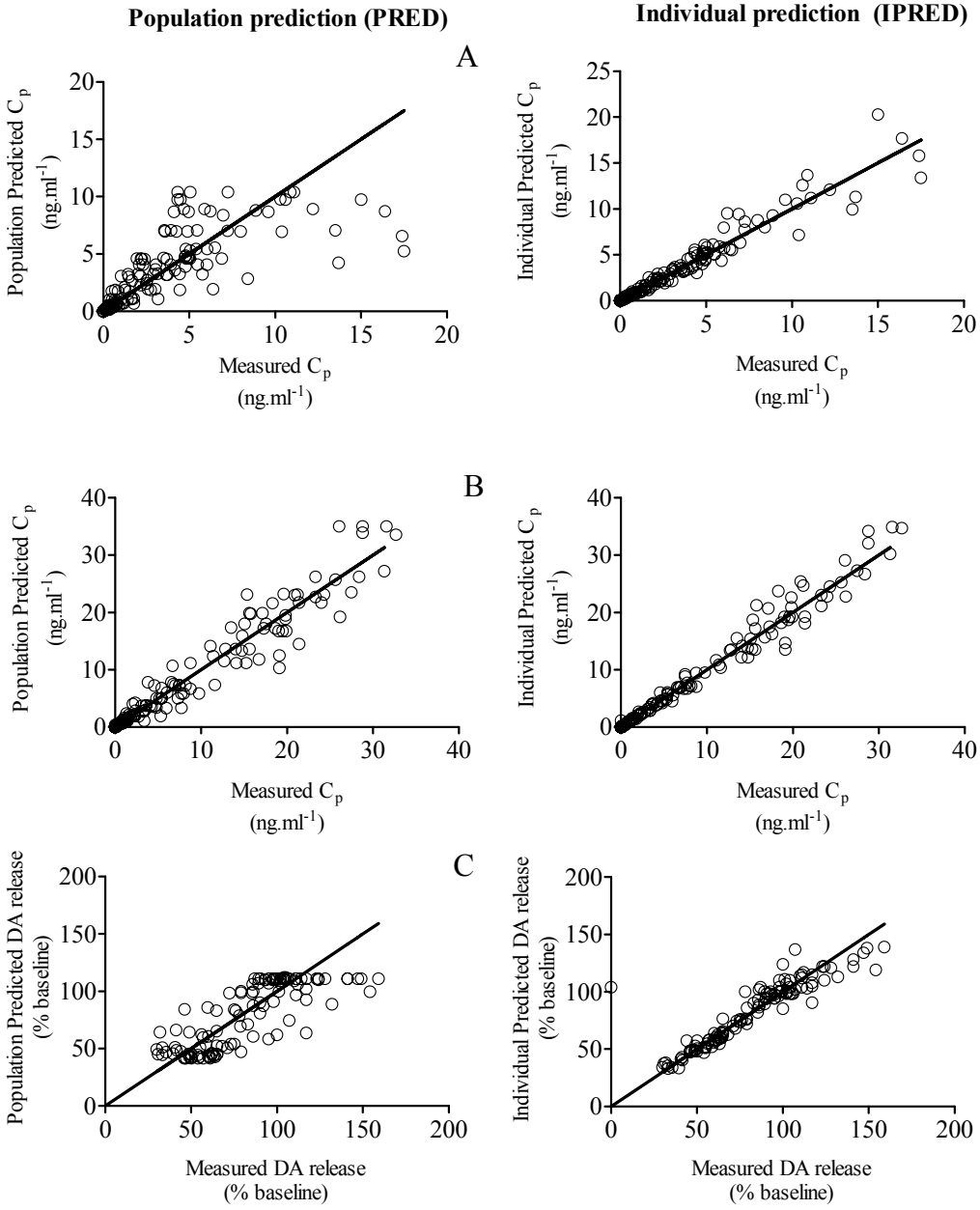

Figure 5: Diagnostic plots of the plasma and striatum analysis using the integrated PK-PD model. **A**: Analysis of plasma concentration (C_p) of (S)-5-OH-DPAT following IV infusion and iontophoresis during the PK study. **B**: Analysis of plasma concentration (C_p) of (S)-5-OH-DPAT following IV infusion and iontophoresis during the microdialysis study. **C**: Analysis of dopamine (DA) release in striatum, expressed as % of baseline values, following IV infusion and iontophoresis. In every panel the population prediction (left graph) and individual prediction (right graph) *vs* the measured value is displayed.

The effect of (S)-5-OH-DPAT (striatal dopamine release) was assessed by two pharmacodynamic models. The first model consisted of a turnover model, i.e., with indirect response type I [14], and the second model consisted of an effect compartment and a sigmoid I_{max} model [13]. The AIC of the effect compartment model was lower than the turnover model. In addition, an improved distribution of the observations in the 95% C.I. of the VPC and a lower residual standard error (RSE) of the parameter estimates were observed when fitting the data with the effect compartment model (comparison not shown). Therefore the effect compartment model was selected for further evaluation of the PK-PD relationship of (S)-5-OH-DPAT. Given the small bias observed in the simulated median profiles of DA (Figure 4B and 4C), a covariate analysis was performed, which revealed differences in IC_{50} depending upon the administration route. Incorporation of the route of administration as covariate into the model improved the VPC (Figure 4D and 4E) and the objective function decreased significantly (χ^2-test; $p<0.05$). The resulting parameters are summarized in Table 1. PK and PD parameters were estimated with good precision, as indicated by a relatively low RSE of the parameters (≤26 %).

Figure 4D and 4E depict the 95 C.I. together with the simulated median response when including route of administration as covariate in the model. It can be observed that the model slightly under- and overpredicts the median of the DA release following transdermal iontophoresis and IV infusion, respectively. Nonetheless, 95% of the observations can be found within the boundaries of the confidence interval. Finally, goodness-of-fit plots for the dopamine release (Figure 5C) show that the model accurately predicts the observed DA release for both administration routes.

4 Discussion

The present study provides novel information on the pharmacokinetic and pharmacodynamic properties of the active enantiomer of the potent dopamine agonist (S)-5-OH-DPAT. Specifically, the present investigation focused on the controllability of the transdermal iontophoretic delivery of this compound with regard to the plasma concentration and the dopaminergic activity in the striatum.

4.1 Relationship between current density and plasma profile

With regard to the controllability of the plasma concentration, the relationship between the applied current density and the corresponding plasma profile was investigated. Three different current densities (75, 150 and 250 $\mu A.cm^{-2}$) were applied in 2 different studies. A comparison of the pharmacokinetic parameters of

the PK-study (using two current densities 75, 150 μA.cm^{-2}) and the PK-PD study (applying 250 μA.cm^{-2}) revealed a difference in peripheral volume of distribution (V_3), central (CL) and peripheral clearance (Q). The difference in these pharmacokinetic parameters can be attributed to the difference in recovery period after surgery of the animals in the two studies, rather than due to differences in transport/delivery. For the PK-studies, the animals were allowed to recover for at least 1 week, whereas the PK-PD studies were executed 15-20h post surgery. Similar results were found by Torres-Molina and co-workers, who demonstrated that the placement of a permanent cannula in the jugular vein influences the PK parameters of amoxycilin and antipyrin in rats. The PK parameters depended on the time of execution of the experiment after placement of the cannula [17]. This should be taken into account when designing new experiments, especially with a cross-over design.

Despite the difference in PK parameters between the two studies, a clear linear dependency (R^2=0.999) was observed (Figure 6) between the applied current density and the *in vivo* steady state flux, calculated from the zero order mass input using the following equation [18]:

$$Flux_{ss} = \frac{I_0}{S} \tag{11}$$

In literature, similar results were reported for the iontophoretic delivery *in vivo* of hydromorphone and ropinirole [6, 19]. Moreover, Patel *et al.* recently demonstrated the controllability of the plasma concentration profiles by the current density for zolmitriptan [20]. These results show that, despite differences in PK properties, the drug input into the skin can be controlled very carefully by adjusting the current density. This can be very useful in initiating therapeutic treatment with dopamine agonist, adjusting the dose to the demand of the individual patient.

Based on this relationship between the *in vivo* flux and the current density, the *in vivo* flux, applying a current density of 500 μA.cm^{-2}, was estimated at 174.9 nmol.cm^{-2}.h^{-1}. Despite the interspecies differences, this value differs only 21% from the *in vitro* flux across human stratum corneum (211.9 ± 11.1 nmol.cm^{-2}.h^{-1}), when applying a current density of 500 μA.cm^{-2} [21]. This indicates that *in vitro* transport parameters can be used to predict drug delivery properties *in vivo*, even across species. Regarding the rat skin, iontophoretic transport is frequently comparable with human skin, in which iontophoresis may diminish interspecies variations in *in vitro* skin permeation studies [22-23].

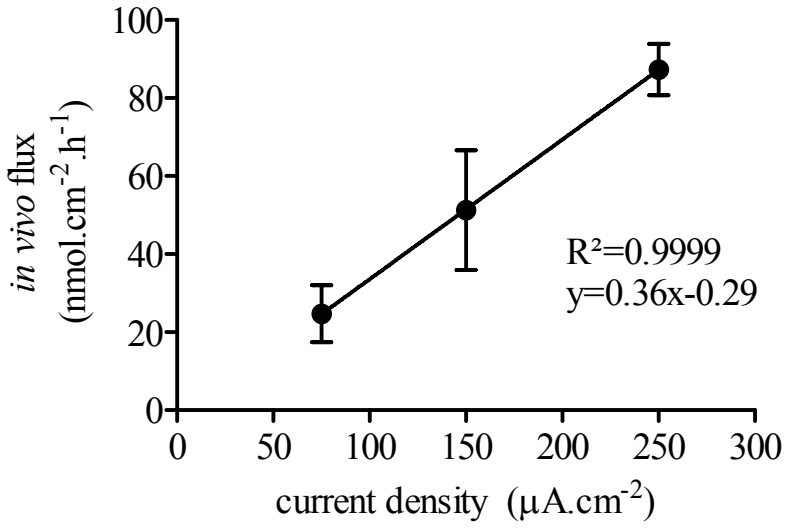

Figure 6: *In vivo* flux *vs* current density. Each data point represents the parameter estimate, determined with compartmental modeling, with the standard error of the parameter estimate. In each experiment 4-6 rats were used.

Our findings suggest the possibility of further refinement of future experiments for the evaluation of drug delivery by iontophoresis. In fact, a model-based approach can be used to to provide guidance for optimal sampling and dose selection as well as by allowing a more quantitative assessment of safety margins. This is one of the reasons why PK-PD modeling is gaining a more prominent place in the different stages of drug development [24].

4.2 PK-PD relationship

Next to a controlled plasma concentration the second aim of our investigation was to characterize the PK-PD relationship of (S)-5-OH-DPAT. A previous study showed that 5-OH-DPAT, administered with transdermal iontophoresis can cause a very strong pharmacodynamic effect. However it was observed that even after 3h post-iontophoresis the dopamine level (PD end-point) did not recover to its initial state [7]. In addition, during these studies choral hydrate was used as anesthetic [7]. Chloral hydrate is not considered the optimal choice for anesthesia of small animals,

like rodents. Moreover several studies showed that choral hydrate influences the striatal DA turnover [25-27] and enhances the suppressive effects of several DA agonists [28]. Therefore our studies were performed following IV infusion and iontophoresis to explore the implications and validate the use of new anesthetic procedures in conjunction with on-line brain microdialysis [10-11]. In addition, we assessed the PK-PD relationship under a wider range of exposures, ensuring reversibility of the PD effect.

A mixture of fentanyl, fluanisone and midazolam was chosen to anesthetize the animals. However, it has been reported in literature that these anesthetics individually also can affect the striatal DA metabolism. Fentanyl and fluanisone can increase the DA turnover in the striatum [29-31], while midazolam has been reported to decrease the DA levels in a dose dependent manner [32]. Besides the effect of the combination of anesthetics, the effect of iontophoresis and blood sampling on the dopamine level was also investigated. As shown in Figure 4A, the stimulating effect of fentanyl and fluanisone and the inhibiting effect of midazolam on the dopamine release were balanced during iontophoresis. After iontophoresis the dopamine release increased slightly, which could indicate a dominating effect of fentanyl. Nonetheless a rat model was established with stable dopamine release levels during anesthesia, which enabled us to investigate the dopaminergic effect of (S)-5-OH-DPAT following intravenous infusion and transdermal iontophoresis.

For both administration routes a decrease in striatal DA level can be observed which returns to baseline within 2h after ending the administration. This demonstrates that a controlled reversible effect can be obtained. Moreover, DA levels seem to reach steady state following transdermal iontophoresis, in parallel to time course of concentrations in plasma. These results suggest that steady state concentrations of (S)-5-OH-DPAT translate into a steady state decrease of the dopamine level. Given that dopamine synthesis is indirectly controlled by presynaptic dopamine receptors, these findings suggest a continuous stimulation of the dopamine receptors [33-34]. Likewise, it has been shown that stable plasma levels of rotigotine, another potent 2-aminotetralin, also result into continuous dopaminergic stimulation [35]. This could be of great benefit for symptomatic treatment of Parkinson's disease. It is generally believed that continuous dopaminergic stimulation is currently the best strategy to reduce motor complications after long-term use of dopaminergic agents [5]. However, further investigations are required applying current for a longer time period with different doses to confirm the applicability of transdermal iontophoresis of dopamine agonists like (S)-5-OH-DPAT.

4.3 PK-PD modeling

The plasma profile and the DA release following IV infusion and transdermal iontophoresis were analyzed using compartmental modeling. Plotting the DA release *vs* the plasma concentration showed a counter clock-wise hysteresis (data not shown). This indicates a time delay between the plasma concentration and the pharmacological response. To account for this delay an effect compartment model [13] was compared with an indirect response model type I [14]. In the present study, it is shown that the DA release is best described by an effect compartment in conjunction with the sigmoidal I_{max} model. This suggests that the delay between plasma concentration and pharmacological response is attributed to the distribution from plasma to site of action, rather than because of a slow onset of the effect. This is further supported by the delayed increase in striatal 5-OH-DPAT concentration following transdermal iontophoresis in Figure 3B. These findings shed light into the mechanisms underlying delay reported by Nugroho *et al.*, who described the DA release, following transdermal iontophoresis of 5-OH-DPAT with an indirect response model type I [7].

As observed in Table 1, the IC_{50} is approximately 2.3 times lower when administering (S)-5-OH-DAT with IV infusion compared to the IC_{50} with transdermal administration. This raises an important question regarding the role of the delivery rate: Do differences in delivery rate alter the response profiles of (S)-5-OH-DPAT? This question can be addressed by estimating the pharmacodynamic efficiency (*EFF*), defined as the pharmacological response per unit of concentration, as shown in the following equation:

$$EFF = \frac{AAEC}{AUC} \tag{12}$$

Where *AUC* (ng.ml^{-1}.min) is the area under the plasma 5-OH-DPAT concentration curve and *AAEC* (DA%.min) is the area above the effect curve (normalized for baseline dopamine levels). For the IV infusion EFF was 9.2 ± 2.3 DA%.ml.ng^{-1}, which is approximately 1.9 ± 0.8 times higher than the EFF following transdermal iontophoresis, estimated at 4.8 ± 1.7 DA%.ml.ng^{-1}. Given that the delivery rate during IV infusion was approximately 3.5 times higher than during transdermal iontophoresis, these observations suggest that a high delivery rate may improve the pharmacodynamic efficiency. In this respect. transdermal iontophoresis can be a suitable delivery technique, since the delivery rate can easily be adjusted using different current densities (Figure 6). For instance a loading dose, by applying a higher current density at the start of the iontophoretic delivery, can be combined with

a maintenance dose, by gradually decreasing the current density to a certain level. Follow-up studies based on drug administration with different delivery rates should be performed to confirm these findings.

The use of an integrated PK-PD approach, simultaneously monitoring drug concentrations in plasma and pharmacodynamic effects, has several benefits over experimental designs in which C_p or the PD effect are evaluated independently. Firstly, it was shown that a steady state plasma concentration may result in a continuous stimulation of the dopamine receptor. Secondly, PK-PD modeling contributes to further understanding of the mechanisms and time course of drug action. Thirdly, PK-PD model parameters can be used to support the design of future experiments. Furthermore, the assessment of PK-PD relationships enables discrimination between delivery-specific and drug-specific parameters. This distinction is critical in drug delivery research, in that it warrants the identification of the factors which may ultimately determine treatment response *in vivo*.

In conclusion, these studies demonstrate that transdermal iontophoresis can be an excellent delivery route for continuous controlled administration of (S)-5-OH-DPAT and other potent dopamine agonists for the symptomatic treatment of Parkinson's disease. PK-PD modeling suggests that target distribution causes the delay between plasma concentration and drug effect. In addition, modulation of the delivery rate seems to have a direct impact on the pharmacodynamics. These results are very important for understanding of the mechanisms underlying drug transport and disposition following transdermal iontophoresis. This information will be crucial for designing a self-controlled delivery device, guided by a feedback system.

Acknowledgements

This research was financially supported by a grant (LKG 6507) of the Dutch Technology Foundation STW, Utrecht, The Netherlands. The authors thank D.J. Vandenberg from the Division of Pharmacology (Leiden/Amsterdam Center for Drug Research, The Netherlands) for the set-up and execution of the analysis of the plasma samples. The authors also acknowledge J.B. De Vries from the Department of biomonitoring and sensoring (University Center of Pharmacy, University of Groningen, The Netherlands) and S.G. Romeijn from the department of Drug Delivery Technology (Leiden/Amsterdam Center for Drug Research, The Netherlands) for their support with the animal studies.

References

1. Dixit, N., et al., *Iontophoresis - an approach for controlled drug delivery: a review.* Curr Drug Deliv, 2007. **4**(1): p. 1-10.
2. Tugwell, C., *Parkinson's disease in focus*. 1st ed. In focus. 2008, London: Pharmaceutical Press. 237.
3. Rajput, A.H., et al., *Clinical-pathological study of levodopa complications.* Mov Disord, 2002. **17**(2): p. 289-96.
4. Syed, N., et al., *Ten years' experience with enteral levodopa infusions for motor fluctuations in Parkinson's disease.* Mov Disord, 1998. **13**(2): p. 336-8.
5. Steiger, M., *Constant dopaminergic stimulation by transdermal delivery of dopaminergic drugs: a new treatment paradigm in Parkinson's disease.* Eur J Neurol, 2008. **15**(1): p. 6-15.
6. Luzardo-Alvarez, A., M.B. Delgado-Charro, and J. Blanco-Mendez, *In vivo iontophoretic administration of ropinirole hydrochloride.* J Pharm Sci, 2003. **92**(12): p. 2441-8.
7. Nugroho, A.K., et al., *Pharmacokinetics and pharmacodynamics analysis of transdermal iontophoresis of 5-OH-DPAT in rats: in vitro-in vivo correlation.* J Pharm Sci, 2006. **95**(7): p. 1570-85.
8. van der Geest, R., M. Danhof, and H.E. Bodde, *Iontophoretic delivery of apomorphine. I: In vitro optimization and validation.* Pharm Res, 1997. **14**(12): p. 1798-1803.
9. van der Geest, R., et al., *Iontophoretic delivery of apomorphine II: An in vivo study in patients with Parkinson's disease.* Pharm Res, 1997. **14**(12): p. 1804-1810.
10. Imperato, A. and G. Di Chiara, *Trans-striatal dialysis coupled to reverse phase high performance liquid chromatography with electrochemical detection: a new method for the study of the in vivo release of endogenous dopamine and metabolites.* J Neurosci, 1984. **4**(4): p. 966-77.
11. Westerink, B.H.C., *Monitoring molecules in the consious brain by microdialysis.* Trac-Trends Anal Chem, 1992. **11**: p. 176-182.
12. Wright, P.M., *Population based pharmacokinetic analysis: why do we need it; what is it; and what has it told us about anaesthetics?* Br J Anaesth, 1998. **80**(4): p. 488-501.
13. Holford, N.H. and L.B. Sheiner, *Understanding the dose-effect relationship: clinical application of pharmacokinetic-pharmacodynamic models.* Clin Pharmacokinet, 1981. **6**(6): p. 429-53.
14. Sharma, A. and W.J. Jusko, *Characterization of four basic models of indirect pharmacodynamic responses.* J Pharmacokinet Biopharm, 1996. **24**(6): p. 611-35.
15. Paxinos, G. and C. Watson, *The rat brain in sterotaxic coordinated. Academic Press: Sydney.* 1982.
16. Holford, N., *The Visual Predictive Check-Superiority to Standard Diagnostic (Rorschach) Plots.* PAGE 14, Abstr 738 [www.page-meeting.org/?abstract=738], 2005.
17. Torres-Molina, F., et al., *Influence of permanent cannulation of the jugular vein on pharmacokinetics of amoxycillin and antipyrine in the rat.* Pharm Res, 1992. **9**(12): p. 1587-91.
18. Nugroho, A.K., et al., *Compartmental modeling of transdermal iontophoretic transport II: in vivo model derivation and application.* Pharm Res, 2005. **22**(3): p. 335-46.
19. Padmanabhan, R., et al., *In vitro and in vivo evaluation of transdermal iontophoretic delivery of hydromorphone* J Control Release, 1990. **11**(1-3): p. 123-135.
20. Patel, S.R., et al., *Controlled non-invasive transdermal iontophoretic delivery of zolmitriptan hydrochloride in vitro and in vivo.* Eur J Pharm Biopharm, 2009. **72**(2): p. 304-9.

21. Ackaert, O.W., et al., *Mechanistic studies of the transdermal iontophoretic delivery of 5-OH-DPAT in vitro.* J Pharm Sci, 2010. **99**(1): p. 275-85.
22. Godin, B. and E. Touitou, *Transdermal skin delivery: predictions for humans from in vivo, ex vivo and animal models.* Adv Drug Deliv Rev, 2007. **59**(11): p. 1152-61.
23. Kanikkannan, N., J. Singh, and P. Ramarao, *In vitro transdermal iontophoretic transport of timolol maleate: effect of age and species.* J Control Release, 2001. **71**(1): p. 99-105.
24. Rajman, I., *PK/PD modelling and simulations: utility in drug development.* Drug Discov Today, 2008. **13**(7-8): p. 341-6.
25. Ford, A.P. and C.A. Marsden, *Influence of anaesthetics on rat striatal dopamine metabolism in vivo.* Brain Res, 1986. **379**(1): p. 162-6.
26. Westerink, B.H. and J. Korf, *Comparison of effects of drugs on dopamine metabolism in the substantia nigra and the corpus striatum of rat brain.* Eur J Pharmacol, 1976. **40**(1): p. 131-6.
27. Zhang, W., et al., *Repeated haloperidol administration changes basal release of striatal dopamine and subsequent response to haloperidol challenge.* Brain Res, 1989. **484**(1-2): p. 389-92.
28. Kelland, M.D., A.S. Freeman, and L.A. Chiodo, *Chloral hydrate anesthesia alters the responsiveness of identified midbrain dopamine neurons to dopamine agonist administration.* Synapse, 1989. **3**(1): p. 30-7.
29. Fregnan, G.B. and R. Porta, *A comparison between some biochemical and behavioural effects produced by neuroleptics.* Arzneimittelforschung, 1981. **31**(1): p. 70-4.
30. Freye, E. and K. Kuschinsky, *Effects of fentanyl and droperidol on the dopamine metabolism of the rat striatum.* Pharmacology, 1976. **14**(1): p. 1-7.
31. Milne, B., L. Quintin, and J.F. Pujol, *Fentanyl increases catecholamine oxidation current measured by in vivo voltammetry in the rat striatum.* Can J Anaesth, 1989. **36**(2): p. 155-9.
32. Takada, K., et al., *Effects of midazolam and flunitrazepam on the release of dopamine from rat striatum measured by in vivo microdialysis.* Br J Anaesth, 1993. **70**(2): p. 181-5.
33. Roth, R.H. and M.C. Nowycky, *Nonstriatal dopaminergic neurons: role of presynaptic receptors in the modulation of transmitter synthesis.* Adv Biochem Psychopharmacol, 1977. **16**: p. 465-70.
34. Westfall, T.C., et al., *The role of presynaptic receptors in the release and synthesis of 3H-dopamine by slices of rat striatum.* Naunyn Schmiedebergs Arch Pharmacol, 1976. **292**(3): p. 279-87.
35. Kehr, J., et al., *Continuous delivery of rotigotine decreases extracellular dopamine suggesting continuous receptor stimulation.* J Neural Transm, 2007. **114**(8): p. 1027-31.